ВАК 2024 MODERN ASTRONOMY: FROM THE EARLY UNIVERSE TO EXOPLANETS AND BLACK HOLES
300 years Russian Academy of Sciences

Magnetic reconnection flux in eruptive and confined solar flares

O. Gopasyuk

Crimean Astrophysical Observatory of the Russian Academy of Sciences, Nauchny, Crimea, 298409 Russia

Abstract. The magnetic properties of 59 flare events (38 eruptive and 21 confined) of GOES class M5.0 and above between February 2011 and December 2022 were analyzed. To identify the statistical properties of magnetic reconnection fluxes, we used the observational data from Solar Dynamics Observatory. The flare durations were analyzed using data from the GOES. The correlation between the GOES peak X-ray flux of a flare and magnetic reconnection flux is strong both for confined and eruptive flares. Eruptive flares show statistically larger magnetic reconnection flux and ribbon area than confined flares. The magnetic reconnection flux is strongly correlated with the flare duration. There is an approximately linear relationship between rise and decay times: the longer the rise time, the longer the decay time. We found a relation between the fraction of active regions (ARs) involved in reconnection process and the eruptive character of large flares. The probability that AR-induced flares will be associated with a coronal mass ejection (CME) increases with the fraction of ARs involved in the reconnection.

Keywords: Sun: magnetic fields, flares, coronal mass ejection

DOI: 10.26119/VAK2024.103

1 Introduction

Magnetic reconnection is responsible for the explosive release of energy on the Sun, resulting in solar flares. During magnetic reconnection the transformation of magnetic energy into the kinetic energy of accelerated particles and thermal energy occurs. Flare events associated with observed CMEs are called eruptive flares, while flares not associated with CMEs are called confined flares. A large number of statistical studies have compared magnetic properties of confined and eruptive flares, including total reconnection magnetic flux Φ_{RB} and reconnection rate (e.g., Tschernitz et al. 2018; Kazachenko 2023; Gopasyuk 2024), total unsigned magnetic flux of a flare-hosting AR, Φ_{AR} (Li et al. 2020), fractions of the AR magnetic flux or area swept by flare ribbons, Φ_{RB} and S_{RB}, relative to the total AR flux or area, $\Phi_{\mathrm{RB}}/\Phi_{\mathrm{AR}}$ and $S_{\mathrm{RB}}/S_{\mathrm{AR}}$, respectively (Toriumi et al. 2017; Tschernitz et al. 2018; Gopasyuk 2024).

In this paper, we present the results of a statistical study of total reconnection fluxes, flare ribbon areas, and flare duration for eruptive and confined events. We also derive quantitative connections between the fraction of the ARs involved in reconnection and the eruptive nature of large flares during the period of solar cycle 24 and the growth phase of solar cycle 25.

2 Data and Methods

We examined the magnetic properties of 59 flares (38 eruptive and 21 confined) of GOES class M5.0 and above from data presented by Gopasyuk (2024). We choose events that are sufficiently isolated in time from other events (that is, the FWHM of the GOES X-ray light curves is well-defined). Thus, the eruptive flare SOL2012-03-07T01:14 was excluded from the data. The flares occurred within 40° of the central meridian from February 2011 to December 2022. The magnetic properties of flare ribbons and ARs were calculated by Gopasyuk (2024) based on the sequences of SDO/AIA images in the 1600 Å band and the preflare normal component of the magnetic field was obtained from SDO/HMI vector magnetograms.

We also have used the parent 2-s (1-s) for flares of 2011-2017 (2021-2022) GOES data sampling to define time scales for each event: e-folding rise τ_{rise} and decay τ_{decay} times, and durations at half maximum (FWHM) of the 1 – 8 Å band. We defined τ_{rise} and τ_{decay} using the GOES X-ray flux F_{SXR} and its time derivative $\dot{F}_{\mathrm{SXR}}$ at the half-maximum times from the GOES data as $\tau = F_{\mathrm{SXR}}/\dot{F}_{\mathrm{SXR}}$. Measuring the e-folding decay time at the half-maximum point may systematically miss the longer time scale, if present, but it more accurately reflects the energy of the flare (impulse phase).

3 Statistical Results

Figure 1(a-f) shows plots of the GOES peak X-ray flux versus the ribbon and AR magnetic properties. The correlation between the GOES peak X-ray flux and $\Phi_{\rm RB}$ is strong (the Spearman correlation coefficient $\rm r_s = 0.6(0.7)$ for eruptive (confined) flares, Fig. 1(a)) in agreement with earlier studies (e.g., Kazachenko 2023), implying that larger flares have more magnetic field involved in reconnection. Similarly, the GOES peak X-ray flux shows a high correlation with $S_{\rm RB}$ ($\rm r_s = 0.5(0.6)$ for eruptive (confined) flares, Fig. 1(b)). For a fixed GOES peak X-ray flux, confined and eruptive flares have the same $\Phi_{\rm RB}$ and $S_{\rm RB}$.

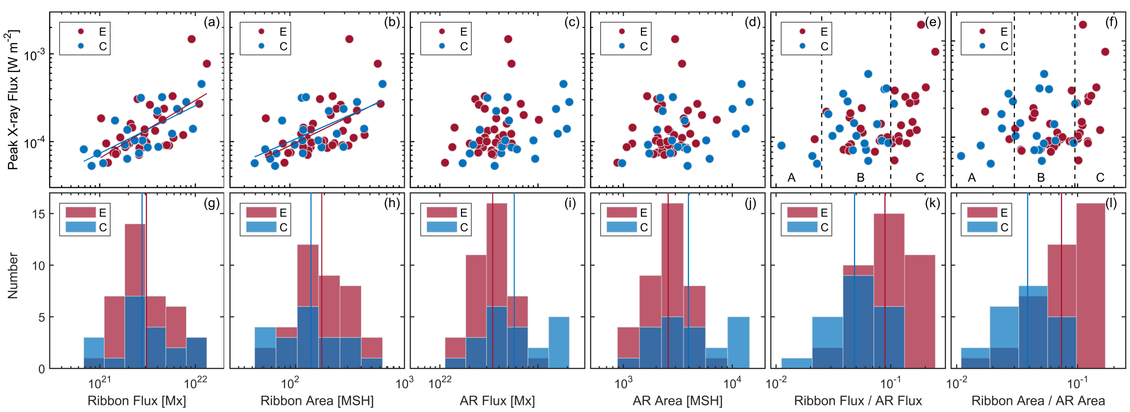

Fig. 1. Scatter plots between the GOES peak X-ray flux and different physical variables (top row), and distributions of various physical variables (bottom row) for eruptive (red) and confined (blue) events. The red and blue straight lines in panels (a–b) show the results of linear fitting for eruptive and confined events respectively. The two dashed vertical lines in panel (e) respectively refer to $\Phi_{\rm RB}/\Phi_{\rm AR}$ of 0.025 and 0.100. The two dashed vertical lines in panel (f) respectively correspond to $S_{\rm RB}/S_{\rm AR}$ of 0.030 and 0.095. Vertical lines in panels (g–l) indicate the log-mean value for each variable within eruptive and confined flare groups.

The correlation between $\Phi_{\rm AR}$ and the GOES peak X-ray flux is weak ($\rm r_s = 0.3(0.4)$ for eruptive (confined) flares, Fig. 1(c)) – larger ARs could host both large and small flares. The AR area $S_{\rm AR}$ and the GOES peak X-ray flux (Fig. 1(d)) also show a weak correlation with a correlation coefficient $\rm r_s$ of 0.3 for both classes of flares. At the same time distributions of magnetic properties (Fig. 1(g–j)) show that $\Phi_{\rm RB}$ and $S_{\rm RB}$ are larger for eruptive flares, while $\Phi_{\rm AR}$ and $S_{\rm AR}$ are larger for confined flares. This leads to the fact that the proportion of ARs involved in reconnection ($\Phi_{\rm RB}/\Phi_{\rm AR}$ and $S_{\rm RB}/S_{\rm AR}$) is higher in eruptive flares (Fig. 1(k–l)).

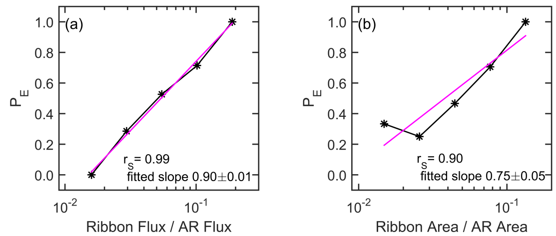

Fig. 2. Proportions of eruptive flares P_E versus Φ_{RB}/Φ_{AR} and S_{RB}/S_{AR}. The magneta lines show the results of linear fitting. Slopes and Spearman correlation coefficients r_s are shown in the lower right corner.

Figure 1(e) shows the scatter plot of the GOES peak X-ray flux versus Φ_{RB}/Φ_{AR}. Flares that are hosted by the ARs with small Φ_{RB}/Φ_{AR} do not generate CMEs (Area A). About 75% of events occurring in ARs with Φ_{RB}/Φ_{AR} less than 0.025 are confined. An overwhelming majority of flares hosted by the ARs with Φ_{RB}/Φ_{AR} higher than 0.100 generate CMEs (Area C). If an AR has a moderate Φ_{RB}/Φ_{AR} (more than 0.025 and less than 0.100, Area B), the probability of eruptive and confined events is apparently almost the same. The scatter plot of the flare peak X-ray flux versus S_{RB}/S_{AR} shows a similar trend (Fig. 1(f)). About 78% of flares in ARs with S_{RB}/S_{AR} less than 0.030 are confined (Area A) and more than 94% flares in the ARs with S_{RB}/S_{AR} more than 0.095 are eruptive (Area C). Approximately equal numbers of confined and eruptive flares occur at intermediate area ratios (0.030–0.095, Area B). Histograms (Fig. 1(k–l)) show that there are significant differences in the distribution of the fraction of ARs involved in reconnection between eruptive and confined flares. Eruptive flares have a large fraction of ARs participating in reconnection. Based on the number distributions of Φ_{RB}/Φ_{AR} and S_{RB}/S_{AR} we show in Fig. 2 the relations of the proportions of eruptive flares P_E ($P_E = N_E/(N_E + N_C)$, N_E and N_C are the numbers of eruptive and confined events respectively) with Φ_{RB}/Φ_{AR} and S_{RB}/S_{AR}. It can be seen that P_E increases with Φ_{RB}/Φ_{AR}. The P_E has a strong correlation with Φ_{RB}/Φ_{AR} with a correlation coefficient r_s of 0.99. Similarly, P_E shows a strong correlation with S_{RB}/S_{AR} ($r_s = 0.90$). This result is similar to the statistical result of Toriumi et al. (2017), who showed the parameter of the ribbon area normalized by the sunspot area determines whether a given flare is eruptive or not. They suggested that the relative structural relationship between the flaring region and the entire AR controls the CME productivity.

In Fig. 3 we analyze how the parameters related to the temporal behavior of the flare (FWHM, τ_{rise}, and τ_{decay}) scale with different physical variables. It can be seen that the dependences do not show significant differences between eruptive and

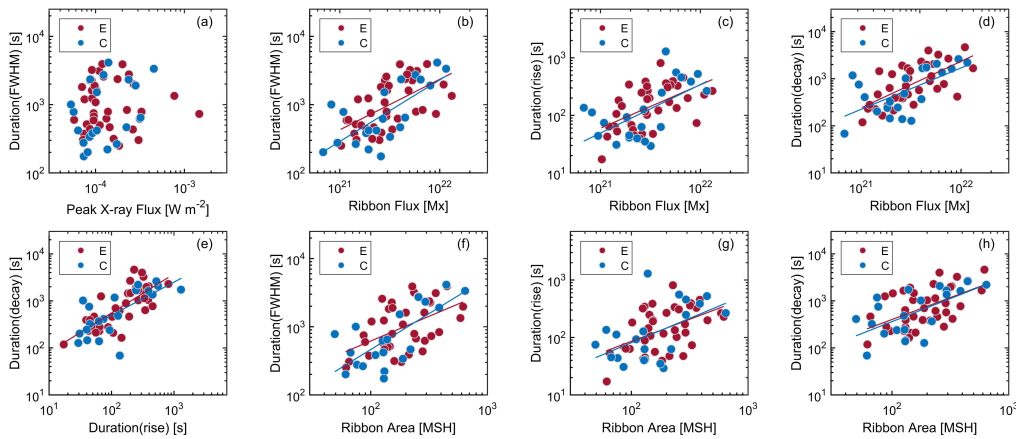

Fig. 3. Scatter plots showing the FWHM, rise and decay times as a function of different physical variables for eruptive (red) and confined (blue) events. The red and blue straight lines show the results of linear fitting respectively for eruptive and confined events.

confined flares. The flare duration FWHM is not related to the GOES peak X-ray flux (Fig. 3(a)). In contrast, the magnetic reconnection flux has a strong correlation with flare temporal parameters, including the duration FWHM ($r_s = 0.6(0.7)$ for eruptive (confined) flares, Fig. 3(b)), $\tau_{\rm rise}$ ($r_s = 0.6(0.5)$ for eruptive (confined) flares, Fig. 3(c)) and $\tau_{\rm decay}$ ($r_s = 0.7$ for both classes of flares, Fig. 3(d)). The relationship between flare duration and $\Phi_{\rm RB}$ shows that the more magnetic flux is involved, the longer the reconnection processes last. The flare ribbon area has a moderate to strong correlation with flare temporal parameters, including the duration FWHM ($r_s = 0.5(0.7)$ for eruptive (confined) flares, Fig. 3(f)), $\tau_{\rm rise}$ ($r_s = 0.4$ for both classes of flares, Fig. 3(g)) and $\tau_{\rm decay}$ ($r_s = 0.5(0.6)$ for eruptive (confined) flares, Fig. 3(h)). The relationship between flare duration and $S_{\rm RB}$ may also be accepted if we assume that the strengths of the field lines are not so different among the events. In Fig. 3(e) we show the decay time versus the rise time. In this case there is an approximate linear relationship between the rise and decay times, with a longer rise time leading to a longer decay time ($r_s = 0.8(0.7)$ for eruptive (confined) flares). However, even in this case, no difference is observed in the behavior of flares with and without a CME.

4 Summary

This paper presents the results of a statistical analysis of the magnetic reconnection flux and duration of 59 (38 eruptive and 21 confined) solar flares with GOES magnitude M5.0 and above based on a dataset compiled by Gopasyuk (2024). The dates of the events cover the period from February 2011 to December 2022, i.e. they practically cover the entire 24th solar cycle and the growth phase of the 25th solar cycle. The main results of our study are as follows.

The correlation between the flare GOES peak X-ray flux and magnetic reconnection flux is strong both for confined and eruptive flares.

We found that the fraction of the AR magnetic flux $\Phi_{\rm RB}/\Phi_{\rm AR}$ involved in the reconnection process plays a significant role in controlling the eruptive nature of flares, and the proportion of eruptive flares exhibits a strong correlation with $\Phi_{\rm RB}/\Phi_{\rm AR}$ ($r_s = 0.99$). About 75% of flares originating from ARs with a ratio magnetic flux less than 0.025 are confined, i.e., they are not associated with a CME. About 100% of events occurring in ARs with $\Phi_{\rm RB}/\Phi_{\rm AR}$ greater than 0.100 are eruptive.

Not all eruptive flares have a long duration. Some flares with CMEs showed a very impulsive rise time, and short durations, and some flares without CMEs were long-duration events. Flare duration (FWHM, $\tau_{\rm rise}$, $\tau_{\rm decay}$) has a moderate to high correlation with $S_{\rm RB}$, and $\Phi_{\rm RB}$ and all these relations showed approximately linear correlations.

Acknowledgements. We acknowledge the GOES and SDO HMI/AIA teams for the availability of the high-quality scientific data.

Funding

This work was supported in the framework of the state assignment on the topic "Research of the Universe objects by observations in radio and optical wavelength ranges" by the Ministry of Science and Higher Education of the Russian Federation under the state registration No. 122022400225-4.

References

Gopasyuk O.S., 2024, Geomagnetism and Aeronomy, 64, 8 in press
Kazachenko M.D., 2023, Astrophysical Journal, 958, 2, id. 104
Li T., Hou Y., Yang S., et al., 2020, Astrophysical Journal, 900, 2, id. 128
Toriumi S., Schrijver C.J., Harra L.K., et al., 2017, Astrophysical Journal, 834, 1, id. 56
Tschernitz J., Veronig A.M., Thalmann J.K., et al., 2018, Astrophysical Journal, 853, 1, id. 41